Simulation of carbonated water injection coreflood experiments

Elsevier Editorial System(tm) for Fuel
Manuscript Draft

Manuscript Number: JFUE-D-16-01367R1

Title: Simulation of Carbonated Water Injection Coreflood Experiments: An Insight into the Wettability Effect

Article Type: Research paper

Keywords: Carbonated water injection (CWI); Mass transfer kinetics; Coreflood Experiments; Oil swelling; Wettability

Corresponding Author: Dr. Jalal Foroozesh, Ph.D.

Corresponding Author's Institution: Heriot-Watt University

First Author: Jalal Foroozesh, Ph.D.

Order of Authors: Jalal Foroozesh, Ph.D.; Mahmoud Jamiolahmady, Ph.D.

Abstract: In this paper, our previously developed model (simulator) has been used to simulate and study a different CWI coreflood experiment from the literature performed in a mixed-wet sandstone core. The developed model which was based on mass transfer kinetics had been used before to simulate a coreflood experiment performed in a water-wet sandstone rock. In this paper, a different procedure has been applied for the simulation of CWI in the mixed-wet core. That is, in contrast to the water-wet coreflood test where only mass transfer parameter was tuned, here, both mass transfer parameter and relative permeability curves have been obtained through a history matching experiment applying our genetic algorithm (GA) based optimization program. Furthermore, using the simulation results, it has been observed that in addition to oil swelling and contrary to the water-wet core, wettability alteration is also an important recovery mechanism for the mixed-wet core. The potential of CO2 storage during the mixed-wet CWI coreflood experiment has also been investigated. The results obtained in this paper can help to crosscheck and verify the performance of the developed simulator and also to explore its generic capability. Moreover, the results of this paper gives an insight into different recovery mechanisms contributing during CWI coreflood experiments.

Highlights (for review)

- A CWI coreflood experiment performed in a mixed-wet core is studied mathematically.
- Compared to CWI in a water-wet core, a different simulation procedure is suggested.
- The contribution of both wettability alteration and oil swilling mechanisms is discussed.

Simulation of Carbonated Water Injection Coreflood Experiments: An Insight into the Wettability Effect

Jalal Foroozesh*, Mahmoud Jamiolahmady

Heriot-Watt University, Institute of Petroleum Engineering, Edinburgh, UK

*Corresponding author:

Email: jalal.foroozesh@gmail.com

Tel: +441314513122

Fax: +441314513127

Abstract

In this paper, our previously developed model (simulator) has been used to simulate and study a different CWI coreflood experiment from the literature performed in a mixed-wet sandstone core. The developed model which was based on mass transfer kinetics had been used before to simulate a coreflood experiment performed in a water-wet sandstone rock. In this paper, a different procedure has been applied for the simulation of CWI in the mixed-wet core. That is, in contrast to the water-wet coreflood test where only mass transfer parameter was tuned, here, both mass transfer parameter and relative permeability curves have been obtained through a history matching experiment applying our genetic algorithm (GA) based optimization program. Furthermore, using the simulation results, it has been observed that in addition to oil swelling and contrary to the water-wet core, wettability alteration is also an important recovery mechanism for the mixed-wet core. The potential of CO_2 storage during the mixed-wet CWI coreflood experiment has also been investigated. The results obtained in this paper can help to crosscheck and verify the performance of the developed simulator and also to explore its generic capability. Moreover, the results of this paper gives an insight into different recovery mechanisms contributing during CWI coreflood experiments.

Keywords: Carbonated water injection (CWI); Mass transfer kinetics; Coreflood Experiments; Oil swelling; Wettability

1. Introduction

Carbonated water (CW) injection is a CO_2-EOR method where CO_2 is used efficiently. In carbonated water injection (CWI) technique and compared to conventional water injection (WI), water will be saturated with CO_2 before injecting into oil reservoirs. Upon contact of CW with oil in the reservoir, CO_2 starts migrating to the oil phase due to its higher solubility in hydrocarbons compared to water, which results in a higher oil recovery factor. During CWI, CO_2 stays dissolved in oil and water phases and not as a free phase, therefore it gives a better sweep efficiency compared to the pure CO_2 injection strategy. Moreover, contrary to the pure CO_2 injection strategy, CWI needs less amount of CO_2 making it an attractive CO_2-EOR strategy for offshore fields, where the supply of CO_2 is limited. Furthermore, through CWI and at the end of the injection period, some amount of of CO_2 (as a greenhouse gas) is stored in the reservoir securely as is dissolved in remaining oil and water [1-4]. CWI has been investigated experimentally and mathematically in the literature. Experimental study of CWI has mainly been focused on flooding tests including cores [4-9]and sand packed set-ups[10, 11]. Direct visualization of flow during CWI using high-pressure transparent micro-model set-up (high pressure Hele-Shaw) has also been considered in the literature [4, 12, 13]. All the reported experiments show an increased recovery factor obtained by CW over conventional WI with some CO_2 stored in the system at end of the experiments. The experiments could help to understand the mechanisms involved during CWI. When CO_2 migrates to the oil phase during CWI, it increases the oil volume (oil swelling) and decrease its viscosity, and reduces IFT of water-oil system all resulting in a better recovery factor [4, 5, 12-14]. However the wettability of rock also affect the efficiency of CWI process. Sohrabi et al. [5] preformed a series of CWI coreflood experiments in a water-wet and a mixed-wet aged core.

They observed that under the same conditions, the recovery obtained for the aged core was higher. The change of wettability of the rock in the presence of CO_2 and specifically by carbonated water is reported in the literature. Yang et al.[15] experimentally measured the contact angle of a crude oil-carbonate rock –carbonated brine system at high pressure and temperatures. A change in contact angle (around 20^0) from oil-wet towards intermediate-wet (neutral-wet) due to the presence of CO_2 in the system was observed quickly (in less than 10 minutes). Seyyedi et al.[16]performed a series of contact angle measurements to determine the wettability of three different minerals (substrates) of quartz (the main mineral of sandstone rocks), mica, and calcite (the main mineral of carbonate rocks) in the presence of a crude oil and carbonated brine at reservoir conditions. In addition to clean substrates, the substrates were also aged in the same crude oil to measure the contact angle of aged minerals as well. The aged quartz showed a contact angle change from 76^0 to 61^0 (natural-wet towards water-wet) and for the aged calcite a contact angle change from 144^0 to 97^0 was observed (oil-wet towards neutral-wet) due to CO_2 dissolution in brine. For the unaged minerals, a small change in contact angle was observed (around 5^0 or less). To provide more support to the idea of wettability change during CWI, Seyyedi and Sohrabi [17] performed a series of spontaneous imbibition tests at reservoir conditions using aged and unaged sandstone and carbonate rock samples. No spontaneous imbibition was observed for aged sandstone and carbonate samples when brine was used whereas carbonated water could imbibe into the rock sample. Al-Mutairi et al.[18] measured the wettability of an aged carbonate rock sample under 500 psi pressure and 70 ^{0}C. They observed that the contact angle was changed quickly (in less than one hour) from 101^0 to 83^0 when it was contacted by carbonated water. Wettability alteration by carbonated water has also been observed in micro-model set-up. Based on some observation in a micro-model set-up, Sohrabi et al.[5] realized that the shape of oil ganglia trapped were more rounded after CWI compared to those after WI. They expressed that this difference in shape of oil blobs indicates that the surface of micro-model has become more water-wet after CWI. All these studies show

that the carbonated water can change the wettability of rock surfaces specifically the oil-wet surfaces to neutral-wet surfaces or neutral-wet surfaces to more water-wet surfaces, but it has a minimal effect on water-wet or strong water-wet surfaces. As compared to experimental study, mathematical modeling and simulation of CWI process has not been studied much in the literature. De Nevers[19] presented an analytical model based on the Buckley–Leveret theory to predict the CWI performance. Ramesh and Dixon [20] presented a numerical black-oil based model to predict the performance of Carbone Dioxide (CO_2) flooding and CWI into heterogeneous oil reservoirs. Chang et al.[21] developed a three-dimensional, three-phase compositional simulator to include the impact of CO_2 solubility in water during CO_2 injection. In the compositional model mentioned above, the assumption of instantaneous equilibrium was applied. This assumption implies that in a simulation grid block, distribution of CO_2 between water and oil happens instantly to reach an immediate equilibrium state. Kechut et al.[6] used ECLIPSE300 (E300) commercial software to simulate some available CWI coreflood experiments. They argued that E300 can not properly simulate this process due to intrinsic assumption of instantaneous equilibrium made by E300 which is not valid for CWI coreflood experiments. As mentioned in the literature[22], this assumption can lead to large errors where for example there are short contact times for mass transfer process (laboratory displacement in cores) or large diffusion patterns are available for components to diffuse through them (field scale) and moreover, if there is slow diffusion velocities due to large viscosity of resident fluids. Accordingly, we previously developed a new compositional simulator (model) for simulating CWI process based on mass transfer kinetics where the assumption of instantaneous equilibrium was relaxed[1]. We used the developed model for simulation of a CWI coreflood experiment carried on in an unaged water-wet core. In this article we will use the developed model for simulation of a different CWI coreflood experiment from the literature carried on in an aged mixed-wet core. The simulation results

are interpreted to discover different recovery mechanisms of CWI in water-wet and mixed-wet cores. That is, the main goal here is to explore the role of rock wettability and wettability alteration in the performance of CWI process by considering the experimental data of two cores with different wettabilities. The structure of this paper is: first, a summary of the developed model is presented, next, the results of coreflood experiments are presented and discussed, later the details of simulations and the interpretations of the results are expressed in detail.

2. Mathematical model

A summary of model developed in our previous paper[1] is presented here. The model is one-dimensional, two-phase (oil and water) developed for a system having three components (oil, water and CO_2). The oil phase is a mixture of oil and CO_2 components and the water phase is a mixture of water and CO_2 components. It should be mentioned that during CWI, there is no free CO_2 in the system as all the present CO_2 are dissolved in oil and water phases. The assumptions of no chemical reaction, no gravity effect and having dead oil without any liberated gas in the system are applied. The dead oil is considered as a single pseudo component. The PDE governing equations are continuity equations of each component in the system as given below:

$$\varphi \frac{\partial(\rho\ s\ \omega\ )}{\partial t} = -\frac{\partial(\rho\ u\ \omega\ )}{\partial x} \tag{1a}$$

$$\varphi \frac{\partial\left(\rho\ s\ \omega^{co_2}\right)}{\partial t} = -\frac{\partial\left(\rho\ u\ \omega^{co_2}\right)}{\partial x} + U \tag{1b}$$

$$\varphi \frac{\partial(\rho_w s_w \omega_w^w)}{\partial t} = -\frac{\partial(\rho_w u_w \omega_w^w)}{\partial x} \tag{2a}$$

$$\varphi \frac{\partial(\rho_w s_w \omega_w^{co_2})}{\partial t} = -\frac{\partial\left(\rho_w u_w \omega_w^{co_2}\right)}{\partial x} - U \tag{2b}$$

Eq. (1a) is the continuity equation of the oil component in the oil phase, Eq. (1b) is the continuity equation of the CO_2 component in the oil phase, Eq. (2a) is the continuity equation

of the water component in the water phase and Eq. (2b) is the continuity equation of CO_2 component in the water phase. In the above equations, ω and ω^{co_2} are the mass fraction of oil and CO_2 components in the oil phase, respectively. ω_w^w and $\omega_w^{co_2}$ are the mass fraction of water and CO_2 components in the water phase respectively. s and s_w are the saturation of the oil and water phases, respectively. The summation of the mass fraction of components in each phase and the summation of saturations of oil and water phases are equal to one as a constraint to the above equations. ρ_o and ρ_w are the density (g/cm^3) of the oil and water phases, respectively. $u = -\frac{kKr_o}{\mu_o}\frac{\partial p_o}{\partial x}$ and $u_w = -\frac{kKr_w}{w}\frac{\partial p_w}{\partial x}$ are the Darcy velocity of the oil and water phases, respectively. p and p_w are the oil and ware phase pressures which are related through the capillary pressure function (p_c), i.e., $p_c = p - p_w$. Kr and Kr_w are the relative permeability of oil and water phases, respectively. The Corey correlations shown below are used to define the relative permeability curves [1, 23]:

$$Kr_w=k_{wmax}\, s^{*n_w} \quad , \quad Kr_o=k_{omax}\,(1-s^*)^{n_o} \quad , \quad s^*=\frac{(s_w-s_{wc})}{(1-s_{wc}-s_{or})} \tag{3}$$

The parameters of k_{wmax}, n_w, k_{max}, n_o, s_{or} and s_{wc} will be obtained through a history matching experiment. The 'U' ($g/cm^3/sec$) added on the right hand side of Eqs. (1b) and (2b), expresses the value of the CO_2 mass being transferred from the water into the oil phase as defined below:

$$U = K \times \left(\rho_w \times \omega_w^{co2} \times k_{eq} - \rho \times \omega^{co2}\right) = K \times \left(k_{eq} C_w^{co_2} - C_o^{co_2}\right) \tag{4}$$

where, $K= (k_m \times a)$ with 'k_m' is the overall mass transfer coefficient (cm/sec) and 'a' is the specific interfacial area (1/cm), which is the oil-water interfacial area per unit volume [24]. K (1/sec) which is a pseudo mass transfer coefficient referred as to MTC parameter here. C_w^{co2} and C_o^{co2} are the CO_2 concentration (g/cm^3) in oil and water phases. k_{eq} is the partition coefficient which is defined as $k_{eq}=\frac{C_o^{co_2{}^*}}{C_w^{co_2{}^*}}$ where $C^{co_2{}^*}$ and $C_w^{co_2{}^*}$ are the CO_2 concentration (g/cm^3) in oil and water phases at the equilibrium state. Eq. 4 shows that the rate of CO_2

being transferred is reflected in the MTC parameter and it continues until the CO_2 concentration in the water and oil phases reach equilibrium, i.e. become equal to C^{co_2*} and $C_w^{co_2*}$. The fully implicit finite difference numerical method is used to solve the above PDE equations. The details of the solution technique are given in our previous paper[1].

3. Coreflood Experiments

In our previous paper, a set of WI and CWI coreflood experiment performed in a water-wet (WW) sandstone core was selected from the literature. In this article, a similar set of WI and CWI coreflood experiment but performed in an aged mixed-wet(MW)sandstone core was selected from the same literature[5] to be investigated. The experimental conditions of the both experiments i.e., water-wet and mixed-wet, were the same (2000 psi and 38 ^{0}C). The basic core properties used during the experiments are given in Table 1a. Both of the cores had been fully saturated by n-decane (n-$C_{10}H_{22}$) at 2000 psi and 38 ^{0}C. However, in the case of the mixed-wet core, the same naturally water-wet sandstone core had been aged using a crude oil sample. The fluid properties are given in Table 1b.

Table 1a: Basic properties of the water-wet and mixed-wet cores used during the experimnts[5].

Core	Length (cm)	Diameter (cm)	Porosity (fraction)	Pore Volume(cm^3)	Permeability (mD)
Sandstone - WW	33.2	4.986	0.19	123.16	1300
Sandstone - MW	61.3	4.86	0.16	182	850

Table 1b: Fluid properties [1].

Fluid	Viscosity(cP) (Test conditions) (136.1 atm, 38 ^{0}C)	Density (g/cm^3) (Test conditions) (136.1 atm, 38 ^{0}C)	Density (g/cm^3) Standard conditions (1 atm, 20 ^{0}C)
Decane	0.83	0.730	0.727
Water	0.66	0.995	0.995
CO2	0.067	0.775	0.00184

It was mentioned that [5] the initial water saturation (s_{wi}) had not been established to eliminate any influence it may have on the process. However, we think that the initial water saturation has minimal effect on the CWI performance. This is because the connate water and injected CW would make a single aqueous phase and therefore its presence would have a minimal effect on the mass transfer and CO_2 distribution between phases. However, if pure CO_2 was injected, the initial water saturation could make a resistant layer for the transfer of CO_2 between gas and oil phases. The operational conditions of both experiments are the same given in Table 1c. During the both WI and CWI tests, water or carbonated water (CW) was injected into the core at a constant rate and water and/or decane were collected at a constant pressure at the core outlet. The measured CO_2 content of carbonated water at experimental conditions was 5% (weight percent). Recovery factor (RF) or total oil production (TOP) and differential pressure (DP) across the core versus the injected pore volume (PV) had been recorded during each experiment.

Table 1c: The operational conditions of the coreflood experiments[1].

Injection rate (cm^3/hr)	20
CO_2 mass fraction in injected CW	5 %
Salinity of injected CW (ppm)	10000
Outlet pressure (atm)	136.1
Initial pressure (atm)	136.1
Initial water saturation	0
Temperature (^{0}C)	38

It is worth mentioning that capillary number ($N_c = \frac{u_{df}\,\mu_{df}}{\sigma}$) for the experiment was calculated to be around 9.8 E-8, which is in the range of typical values of capillary number seen in the real oil reservoirs.

Figs. 1a and 1b show RF data of the WI and CWI experiments in the WW and MW cores, respectively plotted versus injected pore volume (PV). Comparing Figs. 1a and 1b, it can be observed that during CWI, oil recovery has improved in both the WW and MW cores. In the WW core, WI and CWI have the same breakthrough point with 64% RF and the final RF of the CWI after 4.1 PV injected is 73% (equivalent to 90 cm^3 oil production) whereas it is 69% (equivalent to 85 cm^3 oil production) for the WI (i.e., 4% additional oil recovery by CWI). That is, 9% additional RF after breakthrough has been obtained by CWI. In the MW core, however, Fig. 1b shows that CWI and WI have different breakthrough points. The final RF of the CWI after 3.3 PV injected is 68% (equivalent to 123.4 cm^3 oil production) while it is 59% (equivalent to 107.7 cm^3 oil production) for the WI (i.e. 9% additional oil recovery by CWI). Moreover, in the MW core, CWI has resulted in 4% additional RF after breakthrough point. It can be concluded that CWI has better performance in the aged MW core. Figs. 2a and 2b compare DP data of the WI and CWI experiments in the WW and MW cores, respectively. Fig. 2a shows that in the WW core, DP data are the same for both the CWI and WI experiments. However, in the MW core, CWI has lower DP in comparison with WI showing an injectivity improvement during CWI (Fig. 2b).

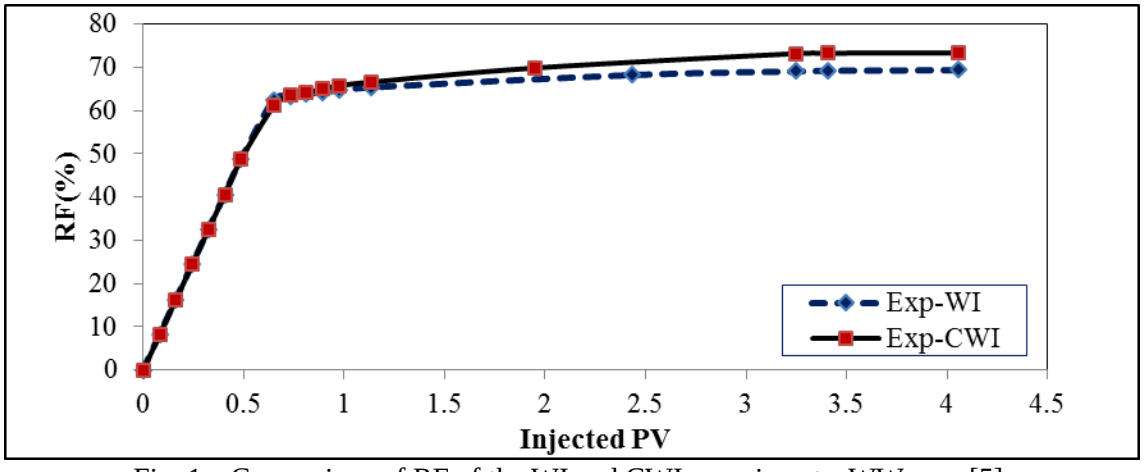

Fig. 1a: Comparison of RF of the WI and CWI experiments, WW core [5].

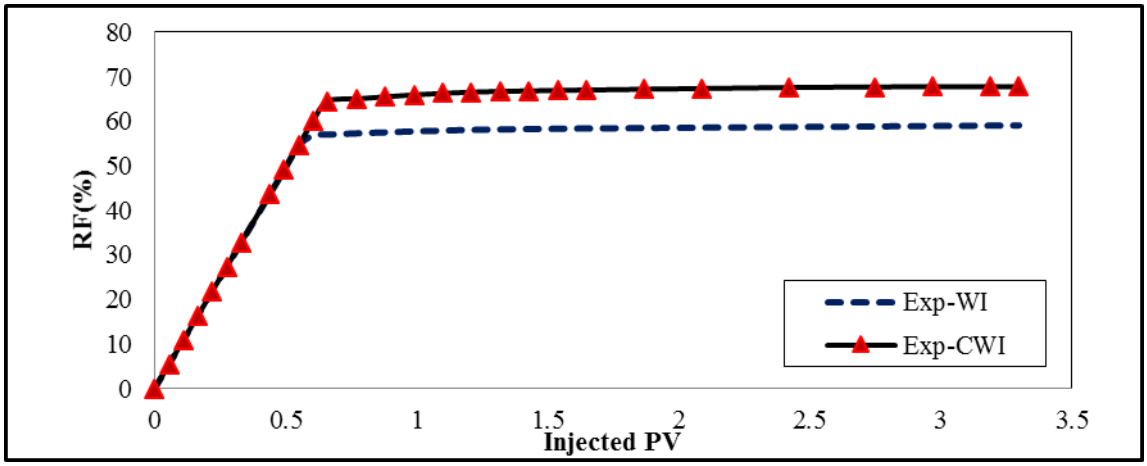

Fig. 1b: Comparison of RF of the WI and CWI experiments, MW core [5].

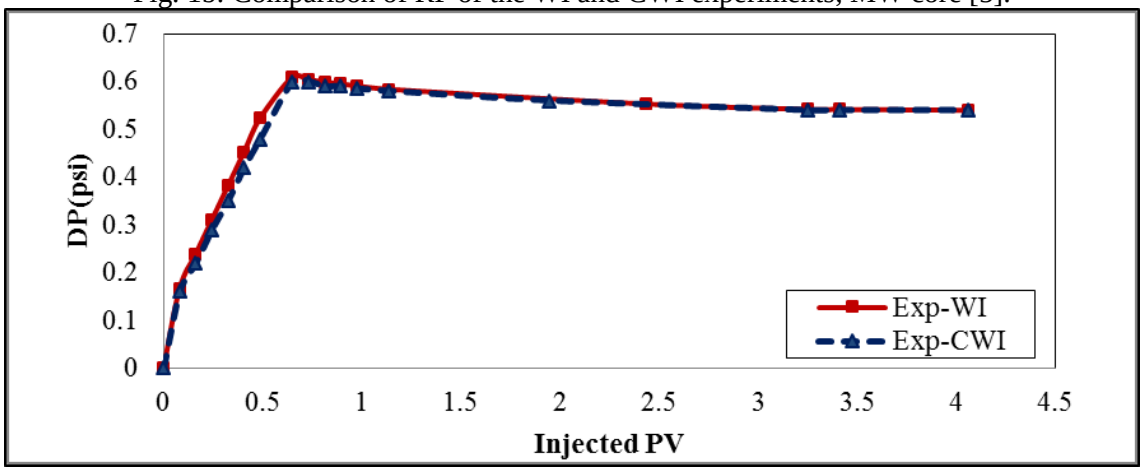

Fig. 2a: Comparison of DP data of the WI and CWI experiments, WW core [5].

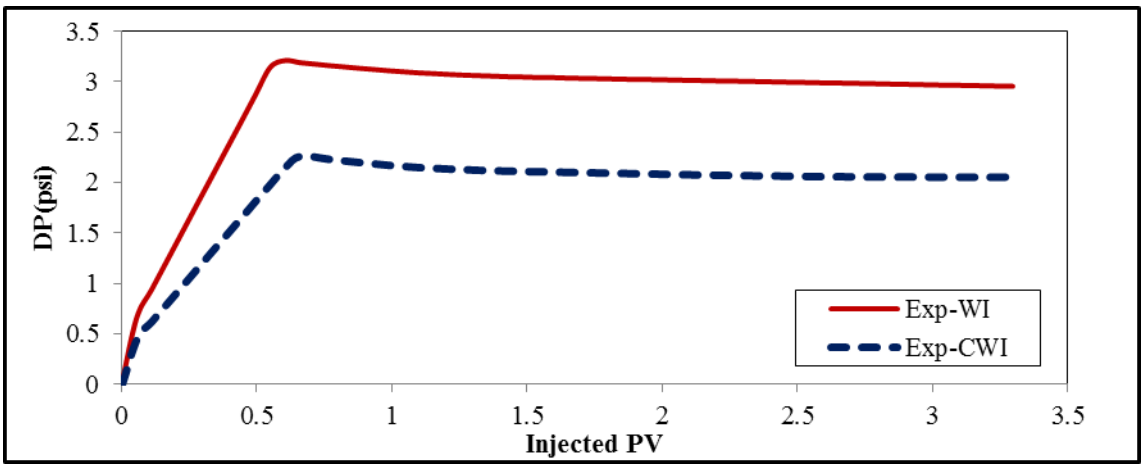

Fig. 2b: Comparison of DP data of the WI and CWI experiments, MW core [5].

4. Results and Discussions

In our previous paper, for the WW core, the WI experiment was simulated first using our developed simulator. The water-oil relative permeability (Kr) and capillary pressure (Pc) based on Corey correlations was obtained through history matching of the WI core

production data applying our GA-based optimization program. Next the CWI experiment was simulated using Kr and Pc from the WI experiment (WI-Kr and WI-Pc). The unknown MTC parameter was obtained by history matching of the CWI production data. The optimal value obtained for MTC was 5E-7 (1/sec). It was discussed and shown that oil swelling was the main mechanism leading to additional oil recovery of CWI over WI in that experiment. An oil swelling factor of 15% was estimated. A similar procedure was followed here to simulate MW coreflood experiments. Initially the WI experiment was history matched using GA program to obtain Corey-based Kr and Pc curves through a history matching experiment. Here, the devolved simulator in its black-oil mode (zero mass transfer and CO_2 concentration) was linked to the GA program. The Corey parameters of Kr curves are k_{wmax}, n_w, K_{omax}, n_o, s_{or} and s_{wc}. The coreflood experiment had been carried out with zero initial water saturation, therefore in the GA program, s_{wc} was set to zero and k_{omax} was set to one accordingly. s_{or} was calculated from material balance and core production data to be 0.41. The k_{wmax} was calculated based on the Darcy equation (shown below) to be 0.074.

$$k_{wmax} = \frac{(\frac{q_{inj}}{A})\times\mu_{water}\times L}{k\times DP_{endpoint}} \quad (1)$$

where q_{inj} is the injection rate, A is the cross section area of the core, μ_w is the water viscosity, L is the core length, k is the absolute permeability and $DP_{endp\ int}$ is the endpoint value on the DP curve. Therefore, the only unknown parameters were n_w and n_o to be optimized. The Pc curve was defined based on the Brooks-Corey correlation[25]. However, for a mixed-wet system, the capillary pressure curve can also be negative [26-28] which cannot be captured by Brooks-Corey correlation. This is because in a mixed-wet rock, some pores are water-wet and some pores are oil-wet and if we define Pc=Pw-Po for all the pores, capillary pressure can also have a negative part. Therefore, Brooks-Corey correlation was modified to predict both positive and negative capillary pressures as follows:

$$Pc=p_{ce}\left(\frac{s_w-s_{wc}}{1-s_{wc}-s_{or}}\right)^{-\frac{1}{\lambda}}-Pcmax/\beta \quad (2)$$

where p_{ce} is the entry capillary pressure (atm), λ is the pore-size distribution index. Pcmax is the maximum Pc (i.e. Pc at connate water saturation) and β is an unknown parameter. In the above equation, the positive term of Pcmax/β shows a fraction of maximum Pc subtracted from the main Brooks-Corey correlation to also have a negative Pc. Similar modification has been suggested in the literature[28]. p_{ce} , λ and β parameters together with n_w and n_o were determined by the GA program. Table 2 shows the initial uncertainty range of each parameter used by the GA during the optimization experiment. These data were selected to be consistent with typical Corey and Brooks-Corey parameters obtained for real oil reservoirs [23].

Table 2: Initial uncertainty range of parameters used in GA.

Kr and Pc parameters	n_w	n_o	p_{ce}(atm)	λ	β
initial uncertainty range	1-5	1-5	0-15	0.2-10	1-25

The misfit (objective function) to be minimised was defined based on summation of absolute relative errors of TOP and DP data ('n' data points) as follows:

$$\text{Misfit}=\sum_{i=1}^{n}\left|\frac{DP_{real}-DP_{predicted}}{DP_{real}}\right|_i+\sum_{i=1}^{n}\left|\frac{TOP_{real}-TOP_{predicted}}{TOP_{real}}\right|_i \quad (3)$$

A minimum misfit of 0.78 has been obtained at the end of the optimisation. The optimal values of the Kr and Pc parameters obtained are summarized in Table 3.

Table 3: The optimal values of the Kr and Pc parameters, WI experiment.

Parameters	n_w	n_o	s_{wc}	p_{ce}(atm)	$\frac{1}{\lambda}$	β
Optimal values	2.5	2.25	0	0.02	0.22	17

Figs. 3 and 4 shows Kr and Pc curves respectively based on the data mentioned above. It is worth mentioning that based on the obtained capillary pressure curve which is positive, perhaps the contribution of water-wet pores has been more dominant. However, another possibility is that after the aging process, the core has changed to be intermediate-wet rather than the mixed-wet and therefore the intermediate wettability might be a more correct term for this core. It can be noted that the capillary pressure is small as the core is homogeneous, with high permeability. Figs. 5a and 5b show the history matched experimental TOP and DP data, respectively.

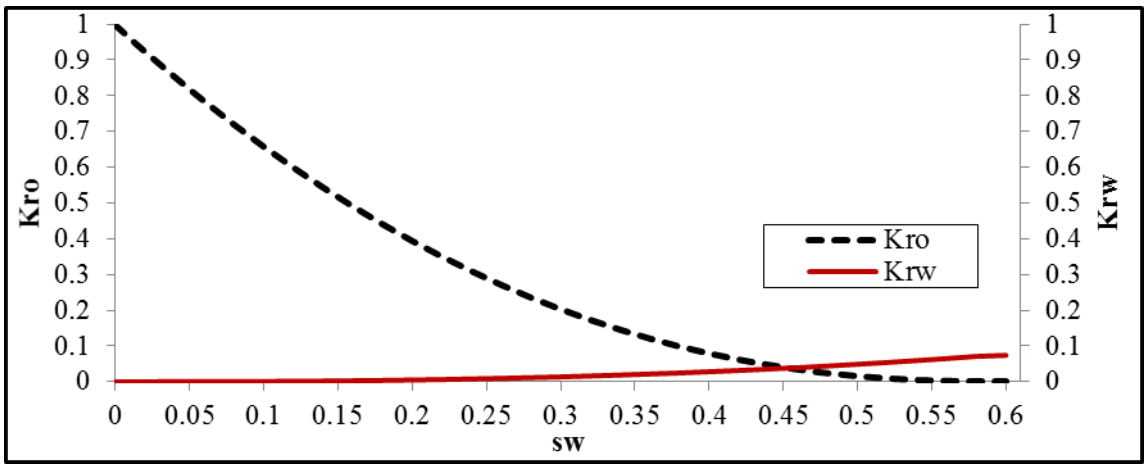

Fig. 3: Optimized Kr_{w-o} curve, WI test.

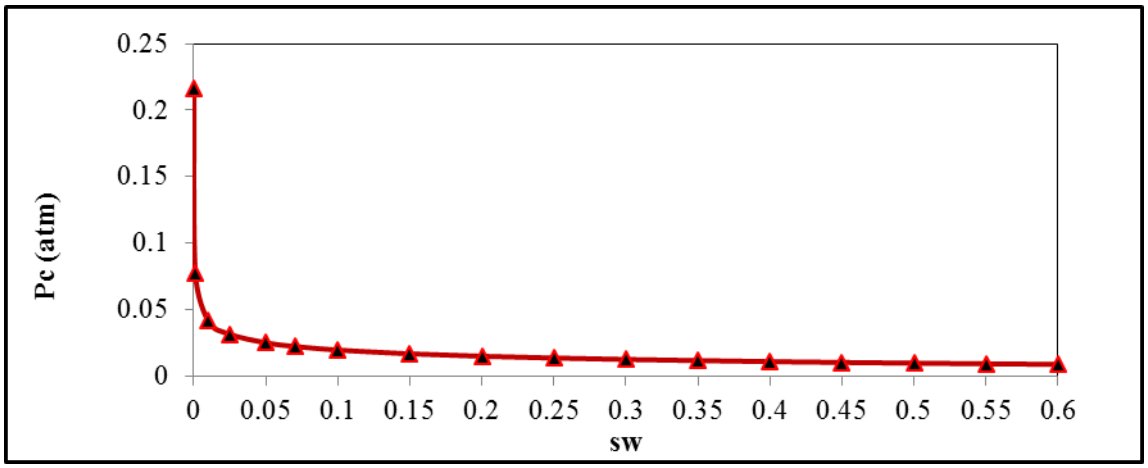

Fig. 4: Optimized Pc curve, WI test.

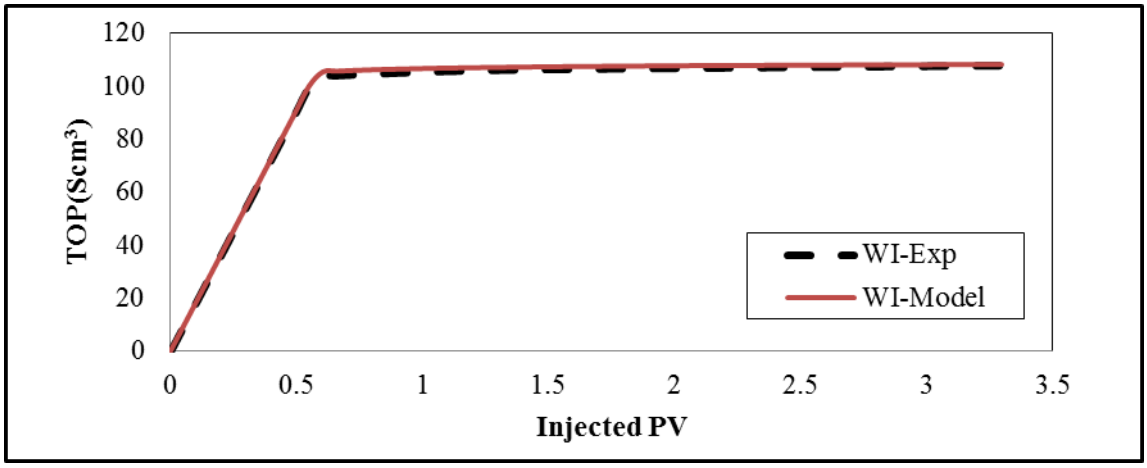

Fig. 5a: History matched TOP-WI data by the developed simulator (model).

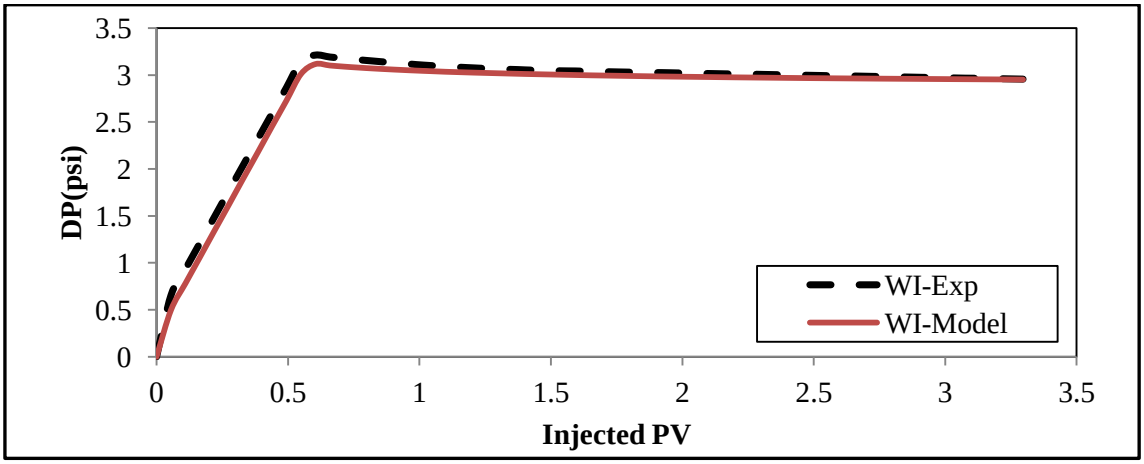

Fig. 5b: History matched DP-WI data by the developed simulator (model).

It is worth mentioning that it was assumed the flow is stable. That is, it was assumed that there is no instability in flow and the discrepancy in flow behavior of water-wet and mixed-wet cores reflected in production curves specifically at breakthrough point is not due to instability in flow i.e. is not due to for example viscous fingering. This is because, the viscosity of water and decane fluids used during test are small and very similar and the core was homogenous. It should be noted that the number of gridblocks in our simulations was optimized to be 200 when further refining of grids did not change the results predicted by the simulator. Moreover, each simulation run took around two minutes to be completed.

Next the simulation of CWI was carried out using the developed simulator in its compositional mode. Initially the MTC and relative permeability curves were unknown. Similar to that for water-wet core, here, first the WI-Kr was used and it was tried to only tune

the MTC value and match the core production data. Figs. 6a and 6b demonstrate the effect of MTC value on TOP and DP data respectively, predicted by the developed simulator (model). Figs. 6a and 6b show that increasing MTC values leads to an increase in the TOP data with minimal effect on DP data while, compared to the WI process, the DP values of the CWI have reduced during the test. Additionally, Fig. 6a shows that the MTC only affects the oil production after breakthrough point and hence the TOP cannot be fully matched if MTC is used as the only unknown parameter of the history matching process to be tuned.

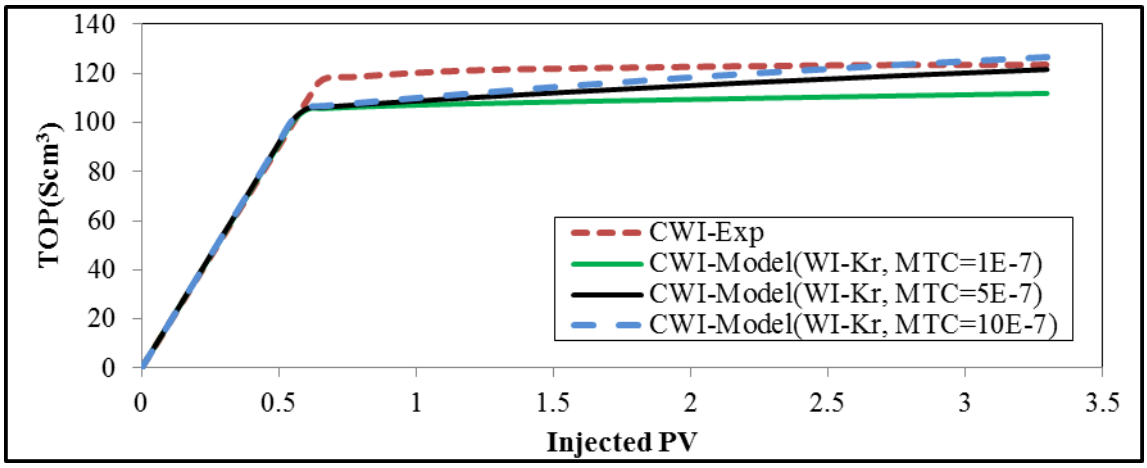

Fig. 6a: Effect of MTC on TOP-CWI data predicted by the model using WI-Kr.

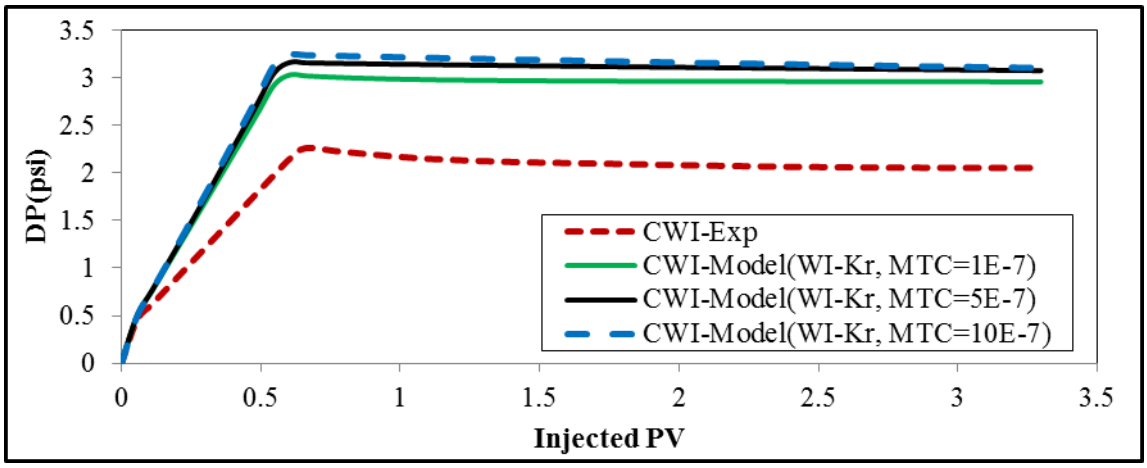

Fig. 6b: Effect of MTC on DP-CWI data predicted by the model using WI-Kr.

Therefore, it was concluded that when using the water-oil relative permeability from the WI experiment, it is not possible to match the CWI experimental data by only tuning the MTC. In other words, both the MTC and relative permeability are needed to be tuned so that the model can predict the experimental data of CWI appropriately. That is, the role and

304 contribution of the mass transfer term in the equations is such that it cannot capture the all
305 mechanisms happing during the CWI process. The mass transfer term contributes mainly
306 towards the oil swelling as it adds some mass to the oil phase, which, in turn, increases the oil
307 volume, resulting in the swelling of the oil. It should be noted that, the viscosity of normal
308 decane is very small (around 0.8cp) and therefore, as discussed in our previous paper, it is not
309 expected that the viscosity reduction to be an important mechanism (viscosity of decane can
310 reduce to around 0.3cp, if it is fully saturated with CO_2). Moreover, as discussed in our
311 previous paper, the level of IFT change between carbonated water and decane fluids is not
312 high making the IFT reduction a negligible recovery mechanism here. To find about the
313 additional mechanisms contributing during CWI, it is worth comparing the TOP and DP data
314 of CWI and WI tests (Figs. 1b and 2b). It can be noted that, the breakthrough point is shifted
315 to the right showing a delayed breakthrough time during CWI and also the DP values have
316 reduced. This may be due to invasion of the carbonated water into the oil-wet pores which are
317 occupied by the oil. The surfaces of these pores are wetted by the oil components and a layer
318 of oil film has adhered to the wall. Carbonated water could probably extract and wash away
319 some part of this oil, i.e. the oil layer which is adhered to the surface of the pores and thus has
320 led to a reduction of residual oil. This has resulted in more oil recovery with a delayed
321 breakthrough time, and also a reduction in the DP values. If this possible process happens, the
322 DP values decreases as there is a larger area available for the water to pass through the pores
323 (i.e. water mobility improvement). This mechanism, which is not seen in the water-wet core,
324 can be related to the wettability modification (or alteration) of the rock surface, which allows
325 the oil layer to be separated from the surface of the pores and be produced during the CWI
326 process. Wettability alteration by CWI has been reported in the literature as mentioned
327 before. To incorporate this into the simulation, the Kr curve from the WI experiment should

328 be modified to capture the effect of wettability alteration during CWI experiment. That is, for
329 the MW, the Kr curve for the CWI test is not the same as that for the WI experiment.
330 It is important to exclude the oil swelling in the Kr curve in the model as it is going to be
331 reflected in the mass transfer term (MTC parameter). Therefore, the main concern and aim at
332 this stage is to quantify and differentiate the role of the oil swelling mechanism and
333 wettability alteration in the CWI performance. It should be noted that, it is difficult to
334 estimate the oil swelling in this MW coreflood experiment explicitly, as wettability is also
335 changed in this system. Therefore, to quantify the oil swelling here, the WW core data were
336 used here.
337 It was first assumed that the same oil swelling and accordingly the same MTC value as
338 that estimated for the WW core is also valid for the MW coreflood test (i.e. 15% swelling and
339 MTC=5E-7 1/sec). However, Figs. 6a and 6b presented above, shows that only the endpoint
340 of the TOP data is matched using this MTC. It had been shown before that for the WW
341 core[1], the oil swelling mainly contributes to additional oil recovery after the breakthrough
342 point and is inherently captured through MTC parameter in the model. In the MW coreflood
343 experiment, as shown in Fig. 1a and discussed above, 9% additional oil recovery was
344 obtained by CWI at end of the experiment after the breakthrough point. However, in the MW
345 core, the additional oil recovery was 4% (Fig. 1b). Therefore, it seems that the importance of
346 the oil swelling and the magnitude of the MTC in the MW core is not exactly the same as that
347 in the WW core. The MTC value for the MW coreflood experiment can be estimated to be
348 2.2E-7 1/sec, using 9% and 4% additional oil recovery obtained over the breakthrough point
349 during the WW and MW coreflood experiments respectively ($\frac{4}{9}$×5E-7=2.2E-7). Moreover, it
350 should be considered that in the WW coreflood experiment, total pore volume of injected
351 carbonated water was 4.1 while in the MW coreflood experiment it was 3.3. Therefore, the
352 amount of mass transferred and resultant oil swelling in the MW coreflood experiment should

be lower than that in the WW coreflood experiment (i.e. lower than 15%). The oil swelling here can be estimated to be 12%, using 4.1 and 3.3 total injected PV during WW and MW coreflood experiments respectively ($\frac{3.3}{4.1}\times 15\%=12\%$). It should be noted that the suggested procedure for the estimation of MTC and swelling in this MW core, based on the data of the WW core and using the linear relations, is an estimation and it could be verified if more experimental data were available. Nevertheless, to support this procedure more, a similar MTC has been obtained from a different method as discussed later on.

To match the TOP and DP data, first the residual oil saturation is adjusted to capture the swelling mechanism. Using the experimental data and based on the material balance, the calculated residual oil saturation (s_{or}) for WI and CWI tests are 0.41 and 0.32, respectively. The 0.32 value is for dead oil saturation, with no CO_2 content and hence, the actual s_{or} should be higher because of its CO_2 content. The estimated oil swelling in this test is 12%. Therefore, the swollen residual oil saturation is estimated to be 36% (32%×1.12=36%). As for the WW core, swollen s_{or} and not dead s_{or} needs to be used in the Kr curve and the difference should be captured by the MTC parameter. Figs. 7a and 7b show, respectively, the TOP and DP data when the s_{or} in WI-Kr is reduced from 41% to 36% and the MTC is set to 2.2E-7 1/sec.

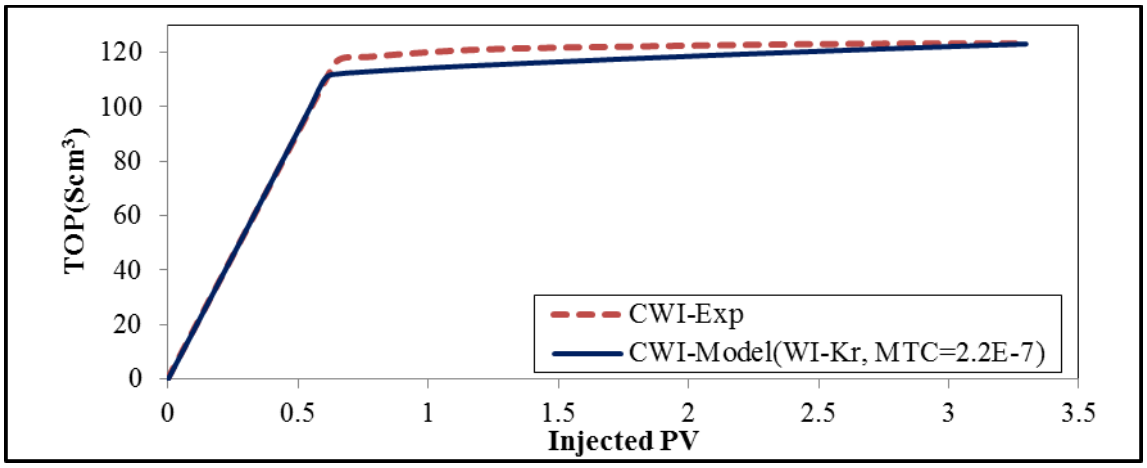

Fig. 7a: TOP-CWI data from the experiment and from the model when WI-Kr with sor=0.36 was used.

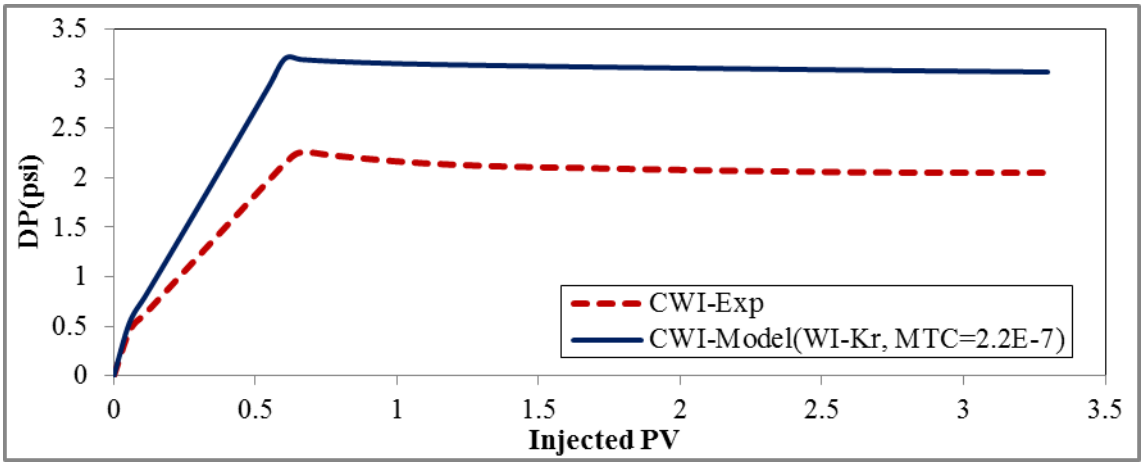

Fig. 7b: DP-CWI data from the experiment and from the model when WI-Kr with s_{or}=0.36 was used.

It can be seen that, at this stage, the TOP data is much closer to the experimental values (compared to Fig. 6a), while predicted DP data are still far away from the experimental data. It seems that the rest of data points on TOP and DP curves need to be matched by tuning the relative permeability curve to capture the wettability alteration effect. The Kr curve can be tuned manually as well as automatically using the GA program. To manually tune the Kr curve, a sensitivity analysis on the Corey type relative permeability curve was performed first. Figs. 8a and 8b are the spider plots, which show the impact of Corey relative permeability parameters on the predicted TOP and DP data, respectively. Fig 8a shows for example, if s_{or} is increased by 25% in the simulator, the predicted TOP decreases by 15%. It can be observed that the TOP data are mainly sensitive to the s_{or} value, whilst the DP data are sensitive to the k_{wmax} value. Moreover, the n_o value affects both TOP and DP data slightly.

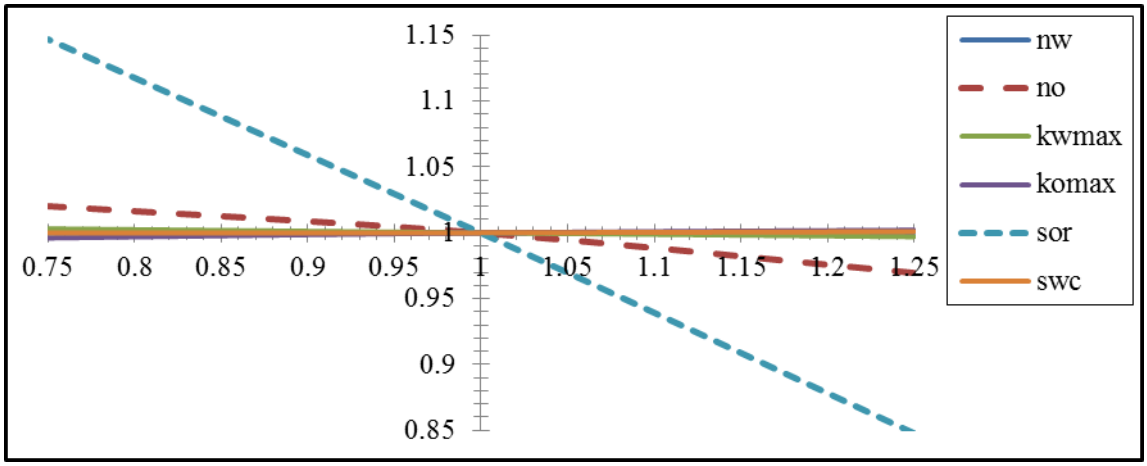

Fig. 8a: Spider plot for TOP.

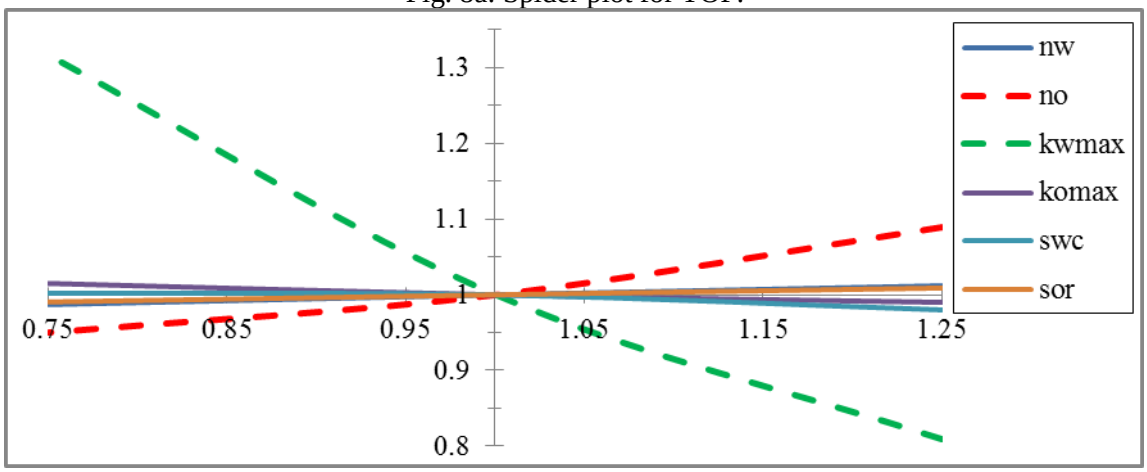

Fig. 8b: Spider plot for DP.

Considering the above results, first the TOP data were matched. To do that, the rest of the TOP data points were history matched by tuning the n_o Corey component and after a few trials, the n_o Corey component from the water injection test was reduced by 25% to have n_o=1.7. It should be noted that a lower n_o value means better oil mobility. Later, the DP data were history matched manually and, after a few trials, k_{wmax} from the water injection test was increased by 36% to have k_{wmax}=0.101. It should be noted that a higher value of k_{wmax} means higher water mobility and it only affects the DP data, as shown during the sensitivity analysis on the Corey parameters. The misfit value of this manual systematic tuning approach was 1.42.

In the second approach, the GA program was used to estimate the optimal values of MTC, k_{wmax}, n_o and s_{or} automatically. It should be noted that in this exercise, the rest of the Corey

parameters were the same as those of the WI test. The minimum misfit value obtained by GA was 1.65. Table 4 compares the optimal parameters of CWI-Kr and MTC obtained by manual tuning and the GA program.

Table 4: Optimal parameters of CWI-Kr and MTC obtained by manual tuning and GA program.

Method	parameters	n_w	n_o	k_{wmax}	k_{omax}	s_{or}	s_{wc}	MTC
	GA	2.5	2.0	0.103	1.0	0.37	0.0	3.0E-7
	Manual tuning	2.5	1.7	0.101	1.0	0.36	0.0	2.2E-7

It can be seen that the values obtained are almost the same supporting the manual tuning procedure suggested above for obtaining the Kr curve. Moreover, this can verify the procedure suggested above to estimate the MTC from WW core data. Figs. 9a and 9b compare respectively the TOP and DP data from the experiments and those predicted by the model using the optimal values of Table 4. It can be seen clearly that the simulator has predicted the TOP and DP data properly.

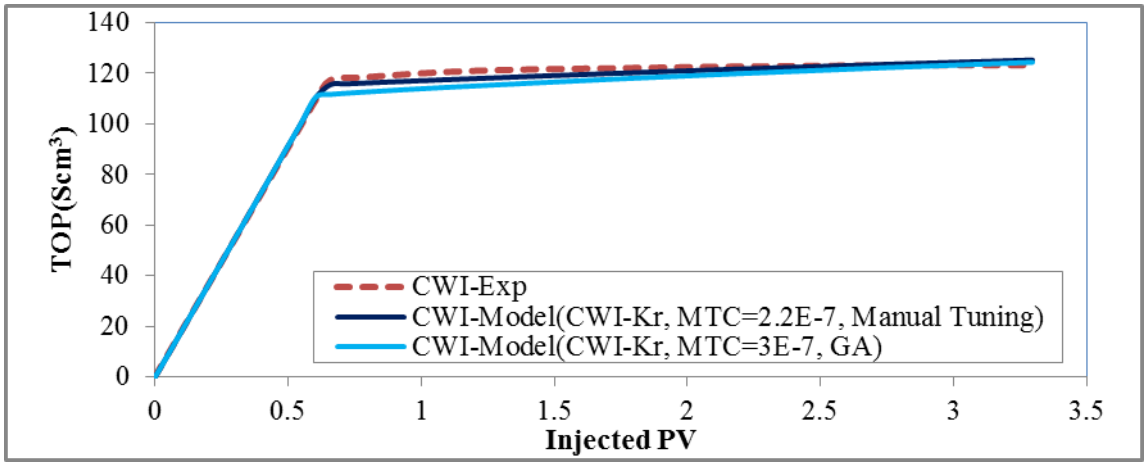

Fig. 9a: TOP-CWI data from the experiment and from the model when optimal parameters by GA and manual tuning (Table 4) was used.

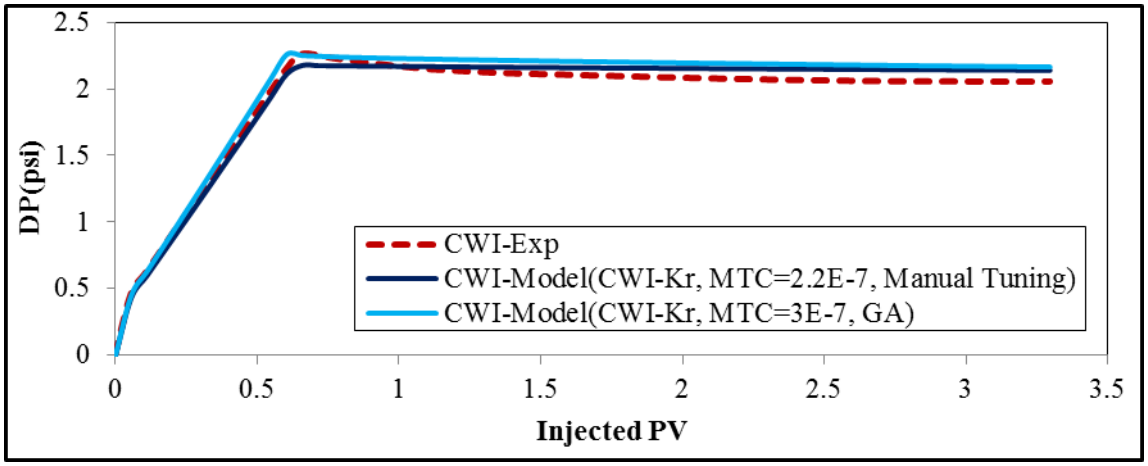

Fig. 9b: DP-CWI data from the experiment and from the model when optimal parameters by GA and manual tuning (Table 4) was used.

It should be noted that during automatic history matching four parameters were optimised simultaneously while during manual tuning, parameters were tuned separately and step by step in a systematic way. This can explain why the misfit value by manual tuning is slightly lower that that by the GA.

In this paper, the results of a coreflood experiment was investigated and simulated. In terms of uncertainty and compared to the real reservoirs, the core properties such as permeability and porosity as input data to the model are associated with less uncertainty. Here, the reported data measured in the laboratory including core properties and the production data have been assumed to be relatively certain. However, if the measurement errors are large, it is expected to be difficult to obtain a close and reliable match between experimental and predicted results. Moreover, perhaps, the main source of uncertainty in this paper are the MTC parameter, Kr curve and Pc curve as these data were obtained through a history matching process. That is, through an inversion process, these input parameters were calibrated such that the simulator could predict the same production data as those from the experiment. Considering the inherent uncertain nature of inversion problems, it is important to carefully consider if the answer is unique and reliable. To reduce the uncertainty in this work, we followed a systematic approach during history matching including a sensitivity

analysis step, manual tuning and GA optimization. In addition, for each experiment, the GA program was run two times to help with reducing the uncertainty of the inversion problem.

Next, similar to the WW core, ECLIPSE300 (E300) compositional simulator was also used here to simulate the CWI process and compare its results with them from our model. A similar E300 model with the same fluid properties and EOS as mentioned in our previous paper was created here. The optimal CWI-Kr obtained above was also used in the E300. Similar to the WW core, E300 over predicted the oil recovery factor. We artificially increased the optimal MTC value obtained above (i.e. 2.2E-7 1/sec) in the model by a factor of 5 and the oil RF predicted by the model increased and became the same as that predicted by E300. It should be mentioned that, in our model, we are able to adjust the amount of CO_2 transfer between the phases however in E300 the CO_2 transfer is imposed by equilibrium criterion.

In next stage, our simulator was used to study the CO_2 storage in the MW core. Fig. 10 compares the CO_2 storage profile (total CO_2 stored (TCO2S) divided by total CO_2 injected (TCO2I) versus injected PV of CW) in the WW and MW cores as predicted by the simulator. It can be seen that after 3.3 PV of CW injected, around 44% of the injected CO_2 has been stored in the MW core while it is around 49% for the WW core. It should be noted that, the CO_2 has stored as it is dissolved in the remaining oil and water in the cores at end of the experiments and as CO_2 solubility in decane is much higher than that in water, CO_2 is mainly in the oil phase inside the cores. As a result, if more oil can be produced due to wettability alteration, more CO_2 will be carried out of the core. This is the reason that a sharper decline can be seen for the MW core in Fig. 10.

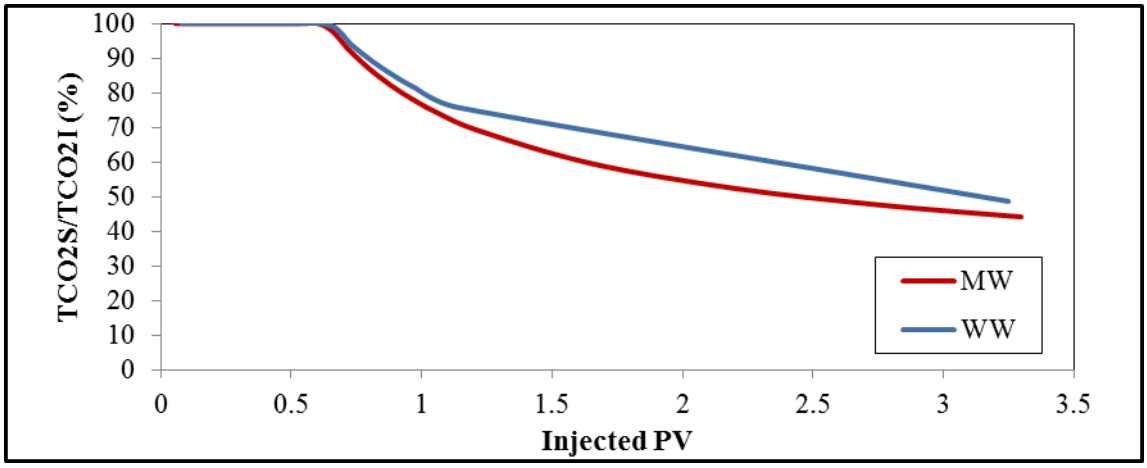

Fig. 10: Comparing ($\frac{TCO2S}{TCO2I} \times 100$) predicted by the simulator in MW with those in WW from our previous paper.

5. Summary and Conclusions

In this work, the previously developed simulator was used to study CWI in an aged MW core. First, experimental data of CWI in the WW and MW cores were compered to gain a better understanding of the the main potential mechanisms. It was noted that CWI in the MW core had a better performance than that in the WW core. In the WW core, DP-WI and DP-CWI data were the same while TOP-CWI data was higher than TOP-WI only after the breakthrough point. This higher oil recovery was attributed to the oil swelling by the CO_2 component. In the WW, DP-CWI data were lower than DP-WI, which was attributed to the wettability wettability alteration. Moreover, the TOP-CWI data were higher than TOP-WI, with a shift in breakthrough point. This shift was also attributed to the wettability alteration. Furthermore, some oil production after the breakthrough point was observed during CWI experiment, which was explained as the effect of oil swelling. Next, WI experiment was simulated and history matched when a proper Kr and Pc curve was obtained. To define Pc, Brooks-Corey correlation was modified such that a negative Pc value can also be predicted. However finally a positive Pc was obtained. Next CWI was simulated when WI-Kr and MTC parameter were modified manually and also using GA program to history match the core production data. It was observed that opposed to the WW core, for the MW core studied here,

Kr curve was not the same for both the WI and CWI processes. It was also attempted to quantify the swelling effect and wettability alteration in the model systematically. Moreover CO_2 storage was also considered and it was observed that more CO_2 could be stored in the WW core compared to that in the MW core.

Nomenclatures

ω = Mass fraction of the oil component in the oil-CO_2 mixture

ω^{co2}= Mass fraction of the CO_2 component in the oil-CO_2 mixture

ω_w^{co2}= Mass fraction of the CO_2 component in the water-CO_2 mixture

ω_w^{w}= Mass fraction of the water component in the water-CO_2 mixture

C^{co2}= CO_2 concentration in the oil-CO2 mixture (g/cm^3)

C_w^{co2}= CO_2 concentration in the water-CO2 mixture (g/cm^3)

$C^{co_2{}^*}$ = CO_2 concentration (g/cm^3) in oil phase at the equilibrium state

$C_w^{co_2{}^*}$= CO_2 concentration (g/cm^3) in water phase at the equilibrium state

k_{eq} = Distribution coefficient, here is 9.6 [1].

MTC=Pseudo mass transfer coefficient (MTC) (1/sec)

p= phase pressure (atm)

s=phase saturation

k=absolute permeability (mD)

φ= porosity

μ = Viscosity of the oil-CO_2 mixture at test conditions (cP)

μ_w = Viscosity of the water-CO_2 mixture at test conditions (cP)

μ_{water} = Viscosity of pure water at test conditions (cP)

p_{ce} = entry capillary pressure (atm)

λ= pore-size distribution index

Pcmax = maximum Pc (i.e. Pc at connate water saturation)

β = an unknown parameter in Pc correlation.

$K = (k_m \times a)$ with 'k_m' is the overall mass transfer coefficient (cm/sec) and 'a' is the specific interfacial area (1/cm).

N_c = capillary number

u_{df} = velocity of displacing fluid, here is carbonated water(m/sec)

μ_{df} = viscosity of displacing fluid, here is carbonated water (kg/m.sec)

σ = carbonated water-decane interfacial tension, here is 20E-3 (N/m) [29]

Acknowledgments

This work has been carried out as part of CWI joint industry project (JIP) at Heriot-Watt University. The CWI JIP is equally sponsored by Petrobras, Total, BG Group, Abu Dhabi Company for Onshore Oil Operations (ADCO), Galp Energia and UK Department of Energy & Climate Change (DECC) which is gratefully acknowledged.

References

[1] J. Foroozesh, M. Jamiolahmady, M. Sohrabi, Mathematical modeling of carbonated water injection for EOR and CO_2 storage with a focus on mass transfer kinetics, Fuel, 174 (2016) 325-332.

[2] N.I. Kechut, M. Riazi, M. Sohrabi, M. Jamiolahmady, Tertiary oil recovery and CO_2 Sequestration by carbonated water injection (CWI), in: SPE International Conference on CO_2 Capture, Storage, and Utilization (SPE No. 139667), New Orleans, LA 2010.

[3] M. Riazi, M. Sohrabi, M. Jamiolahmady, S. Ireland, Oil recovery improvement using CO_2-enriched water injection, in: EUROPEC/EAGE Conference and Exhibition (SPE No. 121170), Amsterdam, The Netherlands 2009.

[4] M. Sohrabi, N.I. Kechut, M. Riazi, M. Jamiolahmady, S. Ireland, G. Robertson, Safe storage of CO_2 together with improved oil recovery by CO_2-enriched water injection, Chemical Engineering Research and Design, 89 (2011) 1865-1872.

[5] M. Sohrabi, N.I. Kechut, M. Riazi, M. Jamiolahmady, S. Ireland, G. Robertson, Coreflooding studies to investigate the potential of carbonated water injection as an injection strategy for improved oil recovery and CO_2 storage, Transport in porous media, 91 (2012) 101-121.

[6] N.I. Kechut, M. Jamiolahmady, M. Sohrabi, Numerical simulation of experimental carbonated water injection (CWI) for improved oil recovery and CO_2 storage, Journal of Petroleum Science and Engineering, 77 (2011) 111-120.

[7] A.H. Alizadeh, M. Khishvand, M.A. Ioannidis, M. Piri, Multi-scale experimental study of carbonated water injection: An effective process for mobilization and recovery of trapped oil, Fuel, 132 (2014) 219–235.

[8] M.A. Ahmadi, M. Zeinali Hasanvand, S. Shokrollahzadeh Behbahani, A. Nourmohammad, A. Vahidi, M. Amiri, G. Ahmadi, Effect of operational parameters on the performance of carbonated water injection: Experimental and numerical modeling study, The Journal of Supercritical Fluids, 107 (2016) 542-548.
[9] A. Fathollahi, B. Rostami, Carbonated water injection: Effects of silica nanoparticles and operating pressure, The Canadian Journal of Chemical Engineering, 93 (2015) 1949–1956.
[10] Y. Dong, B. Dindoruk, C. Ishizawa, E.J. Lewis, An experimental investigation of carbonated water flooding, in: SPE Annual Technical Conference and Exhibition (SPE No. 145380), Denver, Colorado, USA 2011.
[11] N. Mosavat, F. Torabi, Performance of secondary carbonated water injection in light oil systems, Industrial & Engineering Chemistry Research, 53 (2013) 1262-1273.
[12] M. Sohrabi, M. Riazi, M. Jamiolahmady, N.I. Kechut, S. Ireland, G. Robertson, Carbonated water injection (CWI)-a productive way of using CO_2 for oil recovery and CO_2 storage, Energy Procedia, 4 (2011) 2192-2199.
[13] M. Riazi, M. Sohrabi, M. Jamiolahmady, Experimental study of pore-scale mechanisms of carbonated water injection, Transport in porous media, 86 (2011) 73-86.
[14] H. Li, S. Zheng, D. Yang, Enhanced Swelling Effect and Viscosity Reduction of Solvent(s)/CO_2/Heavy-Oil Systems, SPE Journal, 18 (2013) 695-707.
[15] D. Yang, Y. Gu, P. ontiwachwuthikul, Wettability Determination of the Crude Oil-Reservoir Brine-Reservoir Rock System with Dissolution of CO_2 at High Pressures and Elevated Temperatures, Energy & Fuels, 22 (2008) 2362–2371.
[16] M. Seyyedi, M. Sohrabi, A. Farzaneh, Investigation of Rock Wettability Alteration by Carbonated Water through Contact Angle Measurements, Energy & Fuels, 29 (2015) 5544-5553.
[17] M. Seyyedi, M. sohrabi, Enhancing Water Imbibition Rate and Oil Recovery by Carbonated Water in Carbonate and Sandstone Rocks, Energy & Fuels, 30 (2016) 285–293.
[18] S.M. Al-Mutairi, S.A. Abu-Khamsin, T.M. Okasha, M.E. Hossain, An experimental investigation of wettability alteration during CO_2 immiscible flooding, Journal of Petroleum Science and Engineering, 120 (2014) 73-77.
[19] N. De Nevers, A calculation method for carbonated water flooding, Society of Petroleum Engineers Journal, 4 (1964) 9-20.
[20] MATLAB Software 2012, Genetic Algorithm Toolbox User's Guide in.
[21] Y.-B. Chang, B.K. Coats, J.S. Nolen, A compositional model for CO_2 floods including CO_2 solubility in water, SPE Reservoir Evaluation & Engineering, 1 (1998) 155-160
[22] S. Embid, O. Rivas, Simulation of Miscible Displacement with Interphase Mass Transfer Resistance, SPE Advanced Technology Series, 2 (1994) 161-168.
[23] T. Ahmed, Reservoir engineering handbook, Golf Professional Publishing 2001.
[24] J. Geller, J. Hunt, Mass transfer from nonaqueous phase organic liquids in water-saturated porous media, Water resources research, 29 (1993) 833-845.
[25] R. Brooks, T. Corey, Hydraulic properties of porous media, Hydraulic Paper No. 3, Colorado State University, Fort Collins, Colorado, (1964) 1–37.
[26] W.G. Anderson, Wettability literature survey- Part 4: effects of wettability on capillary pressure, Journal of Petroleum Technology 39 (1987) 1283-1300.
[27] J.O. Helland, S.M. Skjaeveland, Physically based capillary pressure correlation for mixed-wet reservoirs from bundle-of-tubes model, SPE Journal 11 (2006) 171-180.
[28] S.A. Bradford, F.J. Leij, Fractional wettability effects on two-and three-fluid capillary pressure-saturation relations, Journal of Contaminant Hydrology, 20 (1995) 89-109.
[29] A. Georgiadis, G. Maitland, J. P. Martin Trusler, A. Bismarck, Interfacial tension measurements of the (H2O+n-Decane + CO_2) ternary system at elevated pressures and

temperatures, ACS Publications, Journal of Chemical &Engineering Data, 56 (2011), 4900-4908.